Supplementary information

Molecular insights into carbon dioxide sorption in hydrazone-based covalent organic frameworks with tertiary amine moieties

K. Gottschling,[a,b,c,d] L. Stegbauer,[a,b,c] G. Savasci,[a,b,d] N. A. Prisco,[e] Z. J. Berkson,[e] C. Ochsenfeld,[b,d] B. F. Chmelka,[e] and B. V. Lotsch*[a,b,c,d]

[a] Max Planck Institute for Solid State Research, Heisenbergstraße 1, 70569 Stuttgart, Germany
[b] Department of Chemistry, University of Munich (LMU), Butenandtstraße 5-13, 81377 München, Germany
[c] Nanosystems Initiative Munich (NIM), Schellingstraße 4, 80799 München, Germany
[d] Center for Nanoscience, Schellingstraβe 4, 80799 München, Germany
[e] Department of Chemical Engineering, University of California, Santa Barbara, California 93106, United States

Contents

Section A. Materials and methods

SEM

SEM measurements were performed on a Zeiss Merlin or a VEGA TS 51300MM (TESCAN).

TEM

TEM was performed on a Philips CM30ST (300 kV, LaB6 cathode) with a CMOSS camera F216 (TVIPS). Samples were suspended in butanol and drop-cast onto a lacey carbon film (Plano).

PXRD

PXRD patterns were recorded at room temperature on a Bruker D8 Discovery with Ni-filtered CuKα-radiation (1.5406 Å) and a position-sensitive detector (Lynxeye).

IR

Fourier-transform infrared spectra were measured on a Jasco FT/IR-4100 or a Perkin Elmer Spectrum NX FT-IR System.

Structural models

Structural models were obtained with Materials Studio v6.0.0 Copyright © 2011 Accelrys Software using the Forcite Geometry optimization with Ewald electrostatic and van der Waals summation methods.

Sorption

Sorption measurements were performed on a Quantachrome Instruments Autosorb iQ MP with Argon at 87 K or with CO_2 at 273, 288 or 298 K. Weight percentage was calculated by referencing to sorbent weight.

Quantum-Chemical Calculations

NMR chemical shifts were obtained on B97-2/pcS-2/PBE0-D3/def2-TZVP level of theory[1-6] using the Turbomole[7-8] program package in version 7.0.2 for geometries and the FermiONs++[9-10] program package for the calculation of NMR chemical shifts.

Section B. Synthetic procedures

1,3,5-triformylbenzene was used as purchased. 2,5-diethoxyterephthalohydrazide and 2,4,6-trihydroxybenzene-1,3,5-tricarbaldehyde were synthesized according to known procedures as follows. All reactions were performed under Ar atmosphere with dry solvents and magnetically stirred, unless otherwise noted.

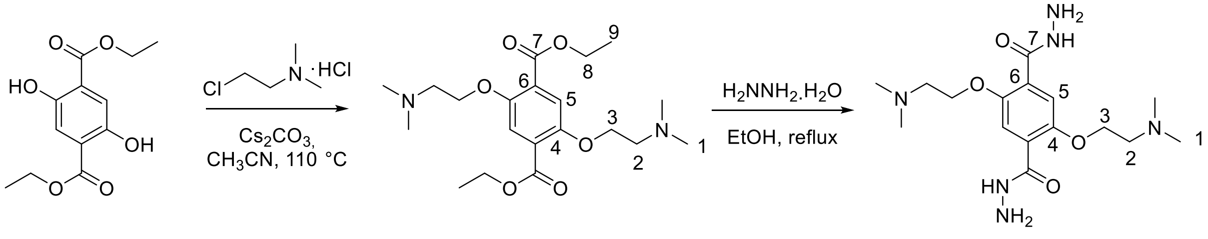

1

2

Diethyl 2,5-bis(2(dimethylamino)ethoxy)terephthalate (1)

Diethyl 2,5-dihydroxyterephthalate (2 mmol, 524 mg, 1 eq) and cesium carbonate (8.4 mmol, 2.74 g, 4.2 eq) were suspended in acetonitrile (20 mL). 2-Dimethylaminoethyl chloride hydrochloride

(4.4 mmol, 640 mg, 2.1 eq) was added. After the reaction mixture was refluxed for 2 h, the solvent was removed. The brownish residue was added into water and extracted with ethyl acetate. The organic extract was dried over magnesium sulfate. The substrate was acidified (HCl 3 m, 3 x 15 mL) and washed with diethyl ether (3 x 15 mL). The mixture was made alkaline with a saturated solution of potassium carbonate in water and extracted with ethyl acetate (3 x 5 mL) until all the organic product was precipitated from the water layer. The organic layer was dried over magnesium sulfate. The solvent was removed to give the product as a light yellow solid (502 mg, 1.27 mmol, 65%).

^{1}H NMR (400 MHz, CDCl$_3$): δ = 7.38 (s, 2H, H$_{\text{arom}}$), 4.36 (q, 4H, Me-CH$_2$), 4.11 (t, 4H, O-C-H$_2$-CH$_2$), 2.75 (t, 4H, N-C-H$_2$-CH$_{2.}$), 2.34 (s, 12H, N-C-H$_{3.}$), 1.38 (t, 6H,O-CH$_2$-C-H$_{3.}$) ppm.

^{13}C NMR (101 MHz, CDCl$_3$): δ = 165.8 (C-7), 152.0 (C-4), 125.2 (C-6), 117.3 (C-5), 68.8 (C-3), 61.5 (C-8), 58.3 (C-2), 46.3 (C-1), 14.4 (C-9) ppm.

^{15}N NMR (400 MHz, CDCl$_3$): δ = -244.5(-NH$_2$), -247.5 (-NH-), -360.3 (-NMe$_2$) ppm.

HRMS (DEI, positive): calc. for $C_{20}H_{33}N_2O_6$ $(M)^+$: 396.2260; found: 396.2256.

IR (FT, ATR): 3801 (br, w), 3076 (br, w, C-H$_{\text{arom}}$), 2939 (m, C-H$_3$), 2820 (w, C-H$_3$), 2660 (br, m), 2416 (m), 1871 (br, m, C=O), 1623 (s, C=C$_{\text{arom}}$), 1496 (w, C-H$_{\text{2deform}}$), 1392 (s), 1368 (s), 1300 (w), 1231 (m), 1205 (m), 1100 (m), 1006 (s), 976 (s), 829 (s, C-H$_{\text{aromdeform}}$), 792 (w), 701 (s), 665 (m) cm^{-1}.

2,5-bis(2-(dimethylamino)ethoxy)terephthalohydrazide (2)

Diethyl 2,5-bis(2-(dimethylamino)ethoxy)terephthalate (0.175 mmol, 70 mg, 1 eq) was suspended in a solution of ethanol/toluene (5 mL, 1:1). Hydrazine hydrate (1.75 mmol, 54.4 µL, 10 eq) was added. The reaction mixture was heated to 110 °C for 8 h. The solvent was evaporated to yield an off-white solid (57 mg, 0.155 mmol, 88%).

^{1}H NMR (400 MHz, CDCl$_3$): δ = 10.52 (s, 2H, N-H), 7.76 (s, 2H, H$_{\text{arom}}$), 4.23 (t, 4H, O-C-H$_2$-CH$_2$), 4.17 (bs, 4H, N-H$_{2.}$), 2.70 (t, 4H, N-C-H$_2$-CH$_{2.}$), 2.33 (s, 12H, N-C-H$_{3.}$) ppm.

^{13}C NMR (101 MHz, CDCl$_3$): δ = 164.8 (C-7), 151.2 (C-4), 125.0 (C-6), 117.4 (C-5), 67.3 (C-3), 57.8 (C-2), 45.1 (C-1) ppm.

HRMS (DEI, positive): calc. for $C_{16}H_{29}N_6O_4$ $(M)^+$: 368.2172; found: 368.2169.

IR (FT, ATR): 3538 (br, m, N-H), 2944 (m, C-H$_3$), 2892 (s), 2820 (m, C-H$_3$), 2772 (m), 2269 (m), 2103 (m), 1647 (m, C=O), 1597 (m, C=C$_{\text{arom}}$), 1487 (m, C-H$_{\text{2deform}}$), 1470 (s), 1417 (w), 1402 (m), 1361 (m), 1302 (m), 1258 (m), 1209 (s), 1161 (m), 1120 (m), 1100 (m), 1063 (m), 1023 (s), 962 (s), 928 (m), 912 (w), 888 (m, C-H$_{\text{aromdeform}}$), 856 (w), 793 (m), 774 (m), 720 (m), 656 (m) cm^{-1}.

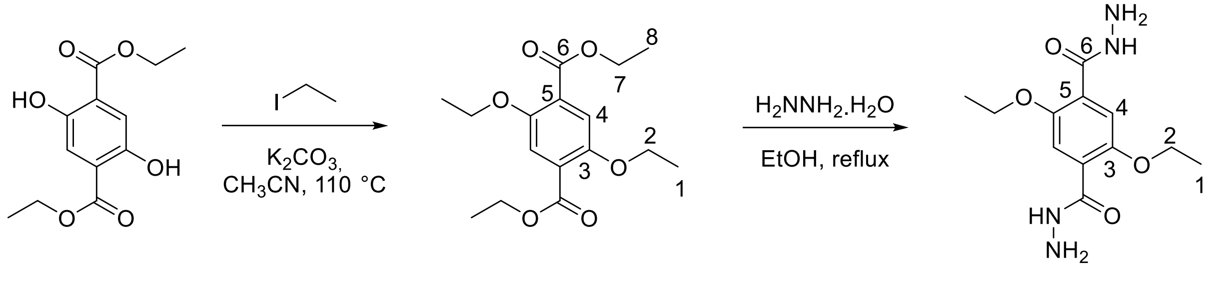

3 **4**

Diethyl 2,5-diethoxyterephthalate (3)

Diethyl 2,5-dihydroxyterephthalate (4 mmol, 1.05 g, 1 eq) and potassium carbonate (13.2 mmol, 1.82 g, 3.3 eq) were suspended in acetonitrile (10 mL). Iodoethane (13.2 mmol, 1.07 mL, 3.3 eq) was added. After the reaction mixture was refluxed for 72 h, the solvent was removed. The brownish residue was

added into water and extracted with ethyl acetate. The organic extract was dried over magnesium sulfate. The solvent was removed to give the product as a light yellow solid (1.20 gg, 3.87 mmol, 97%).
^{1}H NMR (400 MHz, CDCl$_3$): δ = 7.35 (s, 2H, H$_{arom}$), 4.36 (q, 4H, Me-CH$_2$), 4.09 (t, 4H, O-C-H$_2$-CH$_2$), 1.43 (t, 6H, CO-CH$_2$-C-H$_{3.}$).), 1.38 (t, 6H, COO-CH$_2$-C-H$_{3.}$) ppm.

2,5-diethoxyterephthalohydrazide (4)

Diethyl 2,5-diethoxy)terephthalate (3.96 mmol, 1.2 g, 1 eq) was suspended in a solution of ethanol/toluene (20 mL, 1:1). Hydrazine hydrate (39.6 mmol, 1.94 mL, 10 eq) was added. The reaction mixture was heated to 110 °C for 8 h. The solvent was evaporated to yield an off-white solid (903 mg, 3.20 mmol, 81%).
^{1}H NMR (400 MHz, CDCl$_3$): δ = 9.20 (s, 2H, N-H), 7.78 (s, 2H, H$_{arom}$), 4.27 (q, 4H, O-C-H$_2$-CH$_3$), 4.18 (bs, 4H, N-H$_{2.}$), 1.51 (s, 12H, -CH$_{3.}$) ppm.
^{13}C NMR (101 MHz, CDCl$_3$): δ = 163.7 (C-6), 149.5 (C-3), 125.0 (C-5), 114.7 (C-4), 64.8 (C-2), 14.5 (C-1) ppm.
HRMS (DEI, positive): calc. for $C_{16}H_{29}N_6O_4$ (M)$^+$: 282.1328; found: 282.1433.

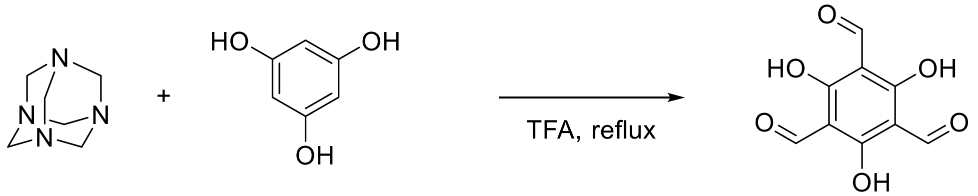

5

2,4,6-trihydroxybenzene-1,3,5-tricarbaldehyde (5)

A solution of hexamethylenetetramine (0.91 mol, 12.9 g, 2.2 eq) and phloroglucinol (0.42 mol, 5.3 g, 1 eq) in trifluoroacetic acid (75 ml) was heated at 100 °C for 2.5 h. 3M HCl (150 mL) was added slowly and heated for 1 h. After cooling to room temperature, the mixture was filtered through a bed of celite. The filtrate was extracted with dichloromethane (4 x 100 mL) and dried over magnesium sulfate. The solvent was evaporated and the residue washed with cold CHCl3 and hot ethanol to yield a light orange solid (2.60 g, 12.3 mmol, 30%).
^{1}H NMR (400 MHz, CDCl$_3$): δ = 14.11 (s, 3H, O-H), 10.15 (s, 3H, -CH=O) ppm.
^{13}C NMR (101 MHz, CDCl$_3$): δ = 192.4 (-CH=O), 174.0 (C-OH), 103.2 (C$_{arom.}$) ppm.

Model compound

N',N''',N'''''-((*1E,1'E,1''E*)-benzene-1,3,5-triyltris(methanylylidene))tri(benzohydrazide) (6)

A mixture of 1,3,5-triformylbenzene (0.27 mmol, 44 mg, 1 eq) and benzoic hydrazide (1.08 mmol, 150 mg, 4 eq) in absolute ethanol (10 ml) was heated at reflux under argon for 4 h. The pale yellow solid separated was collected by filtering the hot heterogeneous reaction mixture and repeatedly washed with ethanol and dried in vacuo (112 mg, 0.22 mmol, 80%).
^{1}H NMR (400 MHz, d_6-DMSO): δ = 12.04 (s, 3H, N-H), 8.57 (s, 3H, N=C-H), 8.13 (s, 3H, H$_{arom.,core}$), 7.94 (d, 6H, H$_{arom.}$), 7.62 (t, 3H, H$_{arom.}$), 7.56 (t, 6H, H$_{arom.}$) ppm.
^{13}C NMR (101 MHz, d_6-DMSO): δ = 163.8 (C-4), 147.0 (C-3), 136.1 (C-2), 133.8 (C-5), 132.4 (C-8), 129.0 (C-1), 128.2 (C-7), 127.1 (C-6) ppm.

HRMS (DEI, positive): calc. for $C_{30}H_{24}N_6O_3$ $(M)^+$: 516.1910; found: 516.1893.

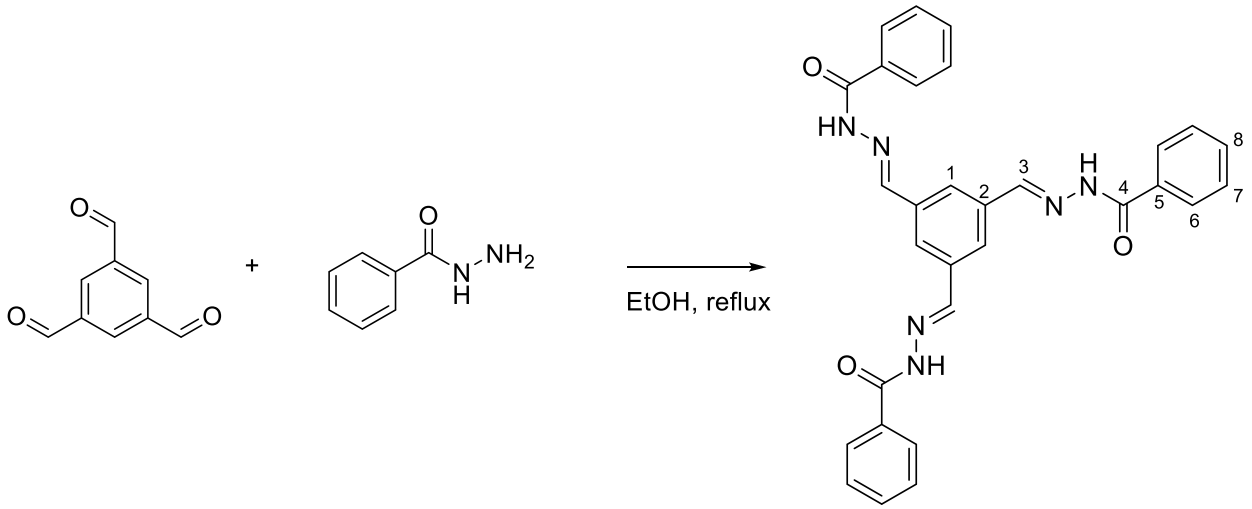

COF synthesis

All products were obtained as fluffy solids. To remove residual starting materials, powders were washed intensely with DMF, THF and dichloromethane and subsequently dried in a vacuum desiccator overnight.

coCOF-H – COF-42

To a Biotage© 2 mL microwave vial, 1,3,5-triformylbenzene (0.066 mmol, 10.7 mg, 2 eq) and 2,5-diethoxyterephthalohydrazide (0.099 mmol, 27.9 mg, 3 eq) were added. Dioxan (0.25 mL), mesitylene (0.75 mL) and acetic acid (6M, 150 µL) were added.. The vial was sealed and heated under microwave irradiation at 160 °C for 30 min. Subsequently, the vial was heated in a muffle furnace at 120 °C for 72 h. After cooling to room temperature, the solid was filtered and washed with DMF (3 x 2 mL), THF (3 x 2 mL) and DCM (3 x 2 mL) to yield a light-yellow powder.

For the copolymerized systems, corresponding amounts of 2,5-diethoxyterephthalohydrazide were replaced by 2,5-bis(2-(dimethylamino)ethoxy)terephthalohydrazide while the procedure was retained as described before. Solvents were used according to Table S1. The products yielded as yellow to orange powders.

coCOF-OH – HTFG-COF

To a Biotage© 5 mL microwave vial, 2,4,6-trihydroxybenzene-1,3,5-tricarbaldehyde (0.132 mmol, 28.6 mg, 2 eq) and 2,5-diethoxyterephthalohydrazide (0.198 mmol, 55.9 mg, 3 eq) were added. Dimethylacetamide (2.25 mL) and 1,2-dichlorbenzene (0.75 mL) and acetic acid (6M, 150 µL) were added. The vial was sealed and heated under microwave irradiation at 160 °C for 30 min. Subsequently the vial was heated in a muffle furnace at 120 °C for 72 h. After cooling to room temperature, the solid was filtered and washed with DMF (3 x 2 mL), THF (3 x 2 mL) and DCM (3 x 2 mL) to yield an orange powder.

For the copolymerized systems, corresponding amounts of 2,5-diethoxyterephthalohydrazide were replaced by 2,5-bis(2-(dimethylamino)ethoxy)terephthalohydrazide while the procedure was retained as described before. Solvents were used according to Table S1. The products were obtained as orange to red powders.

Table S1: Solvent mixtures used in the synthesis of different coCOF-samples.

COF system	Amount of D*t*ATH	Solvent
coCOF-H - COF-42	0%	1,4-dioxane/mesitylene 1:3
	25%	1,4-dioxane/mesitylene 1:1
	50%	*o*-dichlorobenzene/dimethylacetamide 1:3
	75%	1,4-dioxane/mesitylene 1:1
	100%	*o*-dichlorobenzene/dimethylacetamide 1:3
coCOF-OH - HTFG-COF	0%	*o*-dichlorobenzene/dimethylacetamide 1:3
	25%	*o*-dichlorobenzene/dimethylacetamide 1:3
	50%	*o*-dichlorobenzene/dimethylacetamide 1:3
	75%	*o*-dichlorobenzene/dimethylacetamide 1:3
	100%	*o*-dichlorobenzene/dimethylacetamide 1:3

Section C. FTIR spectra

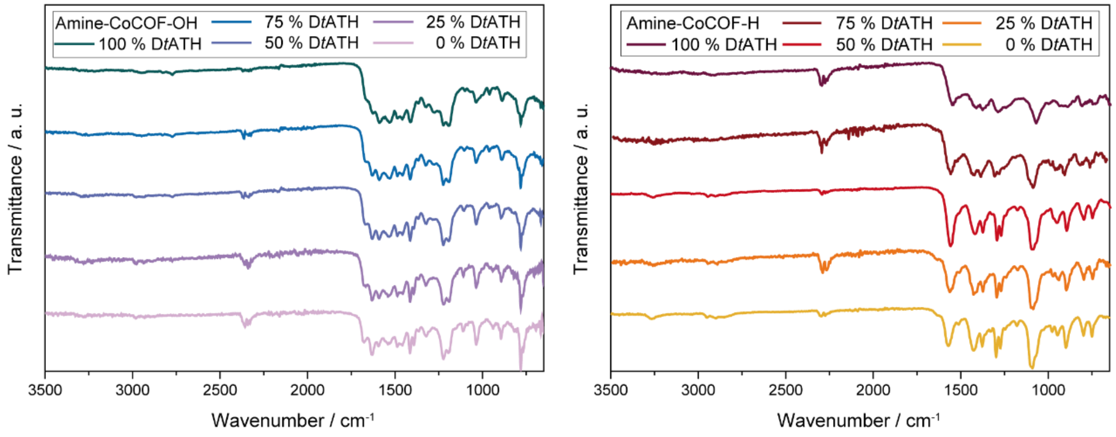

Figure S1: FTIR spectra of Amine-coCOF-OH (left, blue) and Amine-coCOF-H (right, red). Darker color indicates higher amount of D*t*ATH.

Section D. XRD of amine containing samples

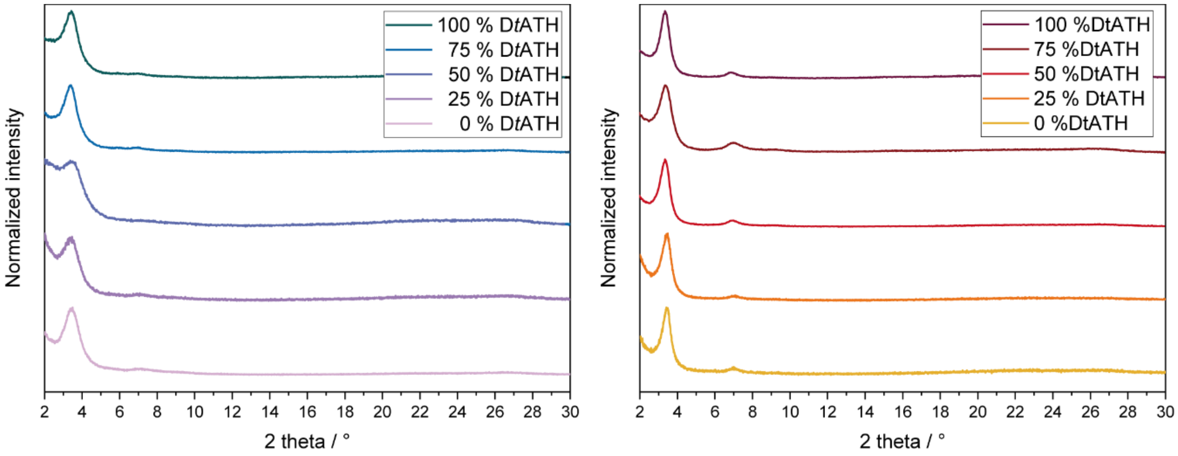

Figure S2: PXRD patterns of Amine-coCOF-OH (left, blue) and Amine-coCOF-H (right, red). Darker color indicates higher amount of D*t*ATH.

Section E. UV/Vis absorption spectra

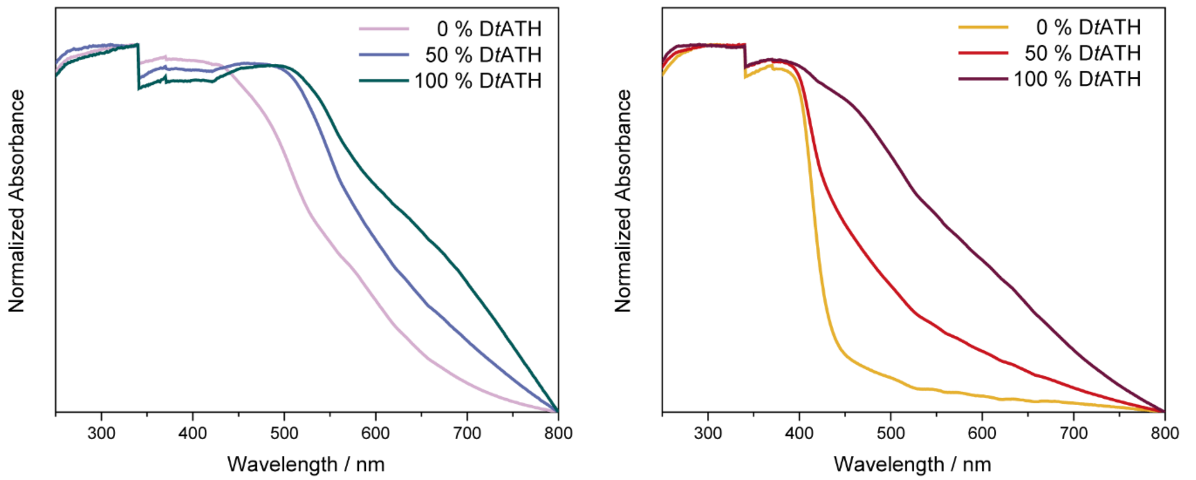

Figure S3: UV/Vis absorption spectra of Amine-coCOF-OH (left, blue) and Amine-coCOF-H (right, red). Darker color indicates higher amount of D*t*ATH.

Section F. Additional sorption measurements

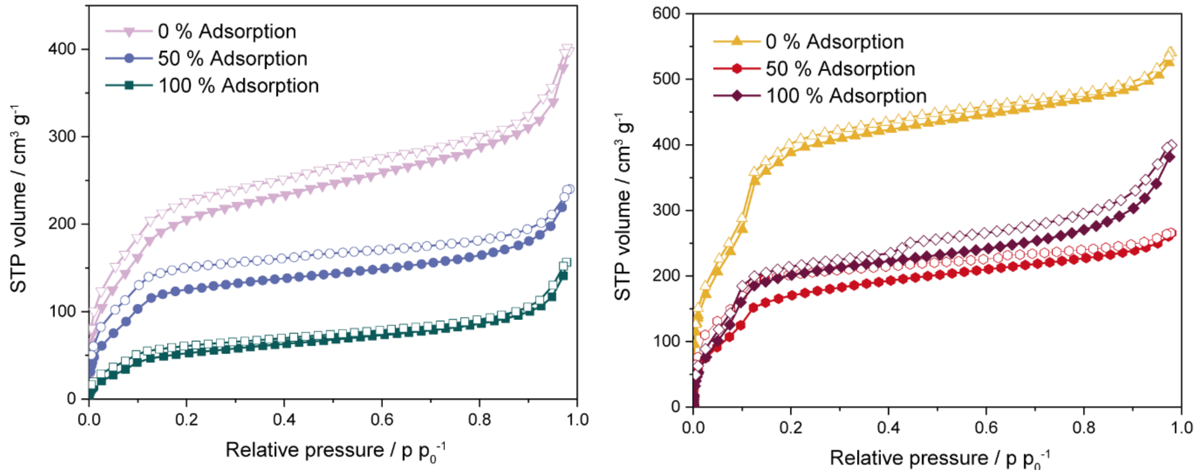

Figure S4: Argon sorption isotherms of Amine-coCOF-OH (left, blue) and Amine-coCOF-H (right, red). Darker color indicates higher amount of DtATH. Adsorption is represented by filled symbols, desorption by open symbols.

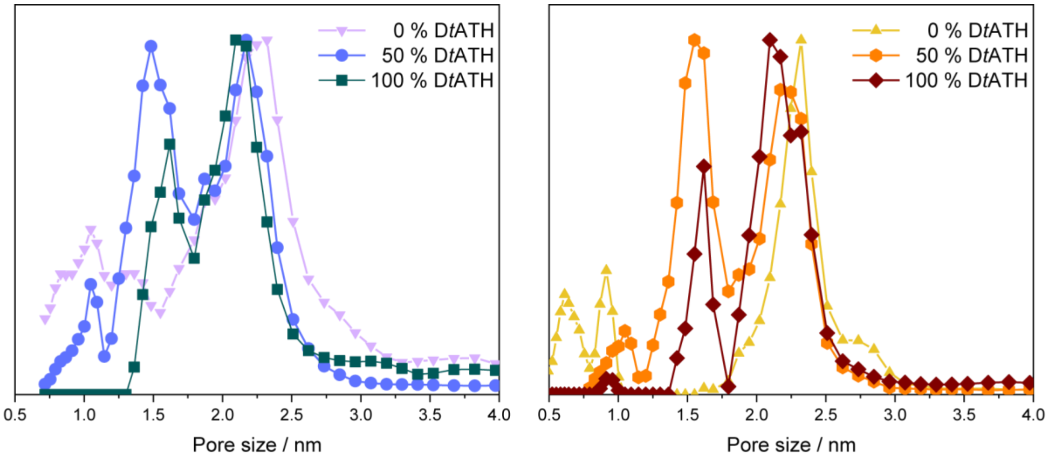

Figure S5: Pore size distribution derived from argon isotherms of Amine-coCOF-OH (left, blue) and Amine-coCOF-H (right, red). Darker color indicates higher amount of D*t*ATH.

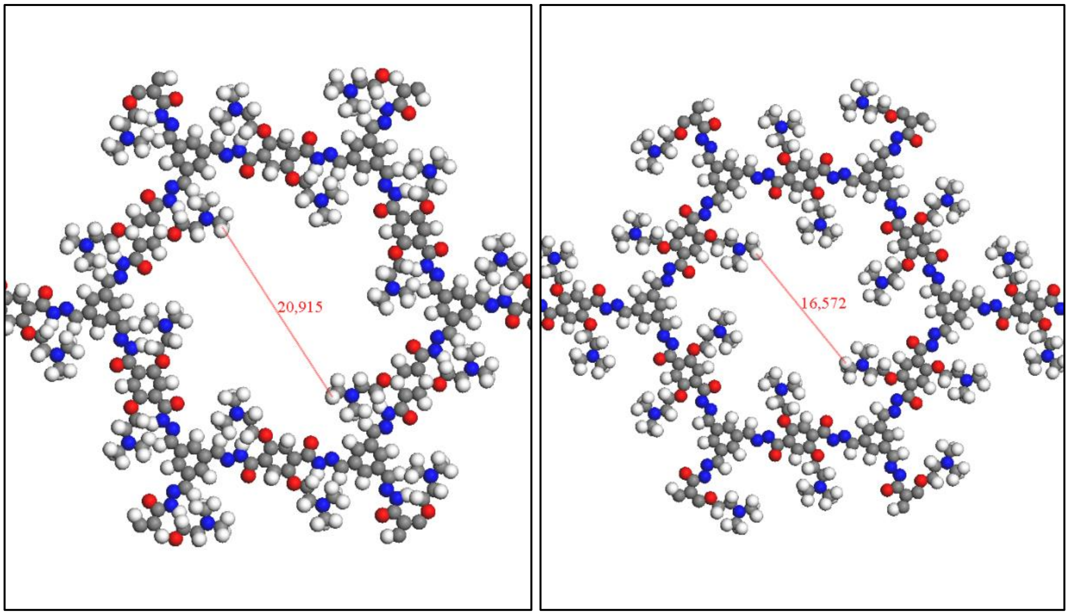

Figure S6: Model for one pore of 100% Amine-coCOF-H. Left: amine side chains at pore walls. Right: amine side chains protruding the pores. C, N, H, and O are represented in grey, blue, white, and red. Smallest pore diameter is marked by red line.

Table S2: Pore sizes, pore volume ($cm^3\ g^{-1}$) and pore volume fractions (%) of the presented COFs.

COF system	Amount of D*t*ATH	Pore size [nm]	Pore volume ($cm^3\ g^{-1}$)	Pore volume fraction (%)[a]
Amine-coCOF-H	0%	2.4	0.28	65
		0.92	0.032	7.4
		0.61	0.036	8.3
	50%	2.24	0.090	36
		1.62	0.067	27
		1.05	0.0067	2.7
	100%	2.09	0.13	59
		1.62	0.04	17
Amine-coCOF-OH	0%	2.3	0.086	55
		0.91	0.041	26
		0.61	0.025	16
	50%	2.17	0.070	39
		1.48	0.052	29
		1.04	0.0073	4.1
	100%	2.16	0.034	56
		1.62	0.0095	16

[a] From 0.0 to 2.7 nm pore size.

Heats of adsorption

Heats of Adsorption were calculated from Henry's law. At low surface excess concentration, the dilute adsorbate phase is treated as a two dimensional ideal gas. The relation is given by

$$n = k_H p$$

Where k_H is the Henry's law constant and n represents the specific surface excess amount. By modeling adsorption in the low-pressure region via a virial-type equation, Henry's law constants can be calculated.

$$\ln\left(\frac{n}{p}\right) = K_0 + K_1 n + K_2 n^2 + \cdots$$

With $k_H = \lim_{n\to 0}(\frac{n}{p})$, Henry's law constant is obtained from the zero-order virial coefficient $K_0 = \ln(K_H)$. With CO_2 adsorption measurements at 273, 287, and 295 K, Henry's law constants for each temperature were identified. The differential enthalpy of adsorption at zero coverage $\Delta\dot{h}_0$ was then calculated from the Van't Hoff equation.

$$\Delta\dot{h}_0 = R\left(\frac{\partial \ln[k_H]}{\partial\left(\frac{1}{T}\right)}\right)_n$$

By plotting $\ln[k_H]$ versus $\frac{1}{T}$ and linearly fitting, the zero coverage enthalpy is equal to the slope of the fit multiplied by the ideal gas constant R.

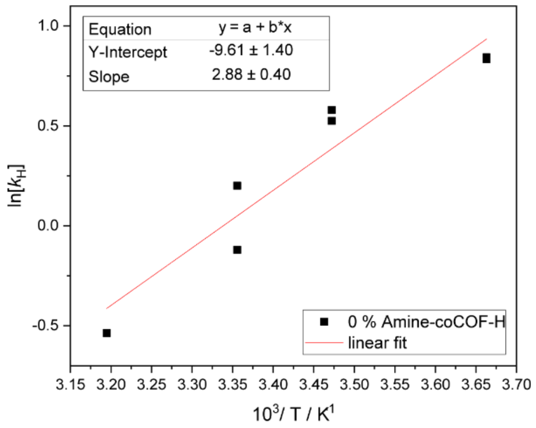

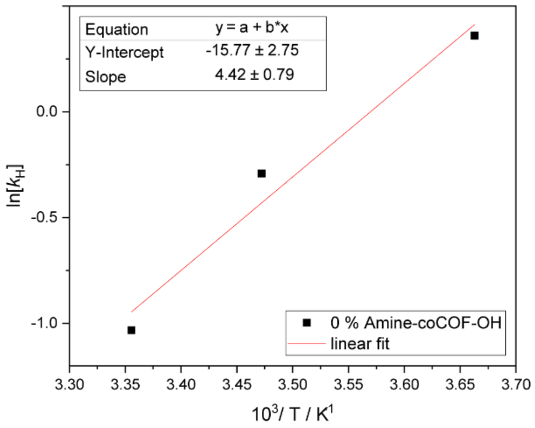

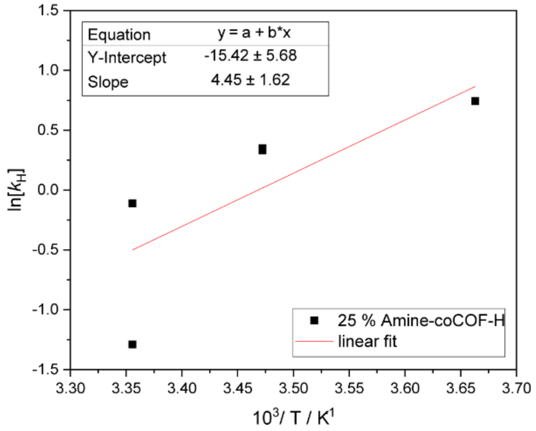

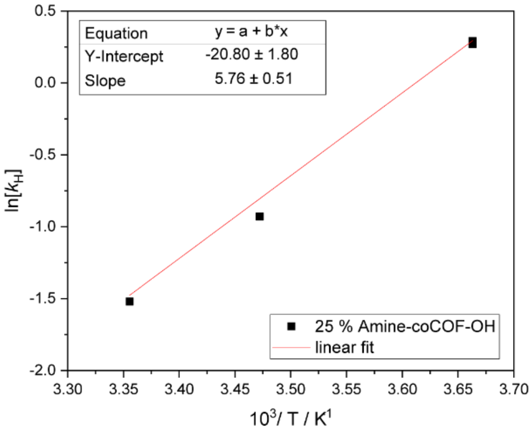

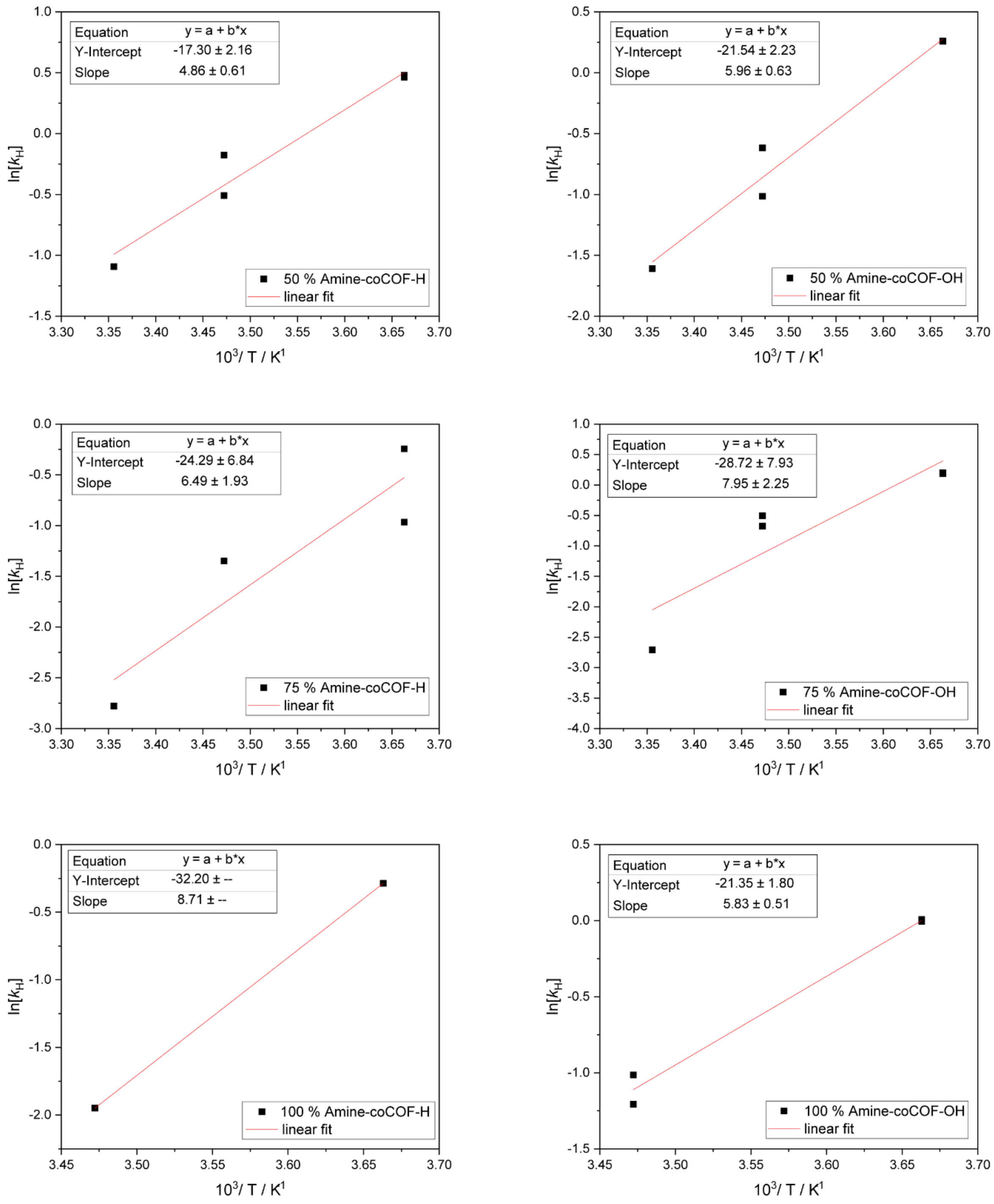

Figure S7: Linear fits of the van’t Hoff equation for the different coCOF-systems and amine amounts.

Section G. Additional NMR measurements

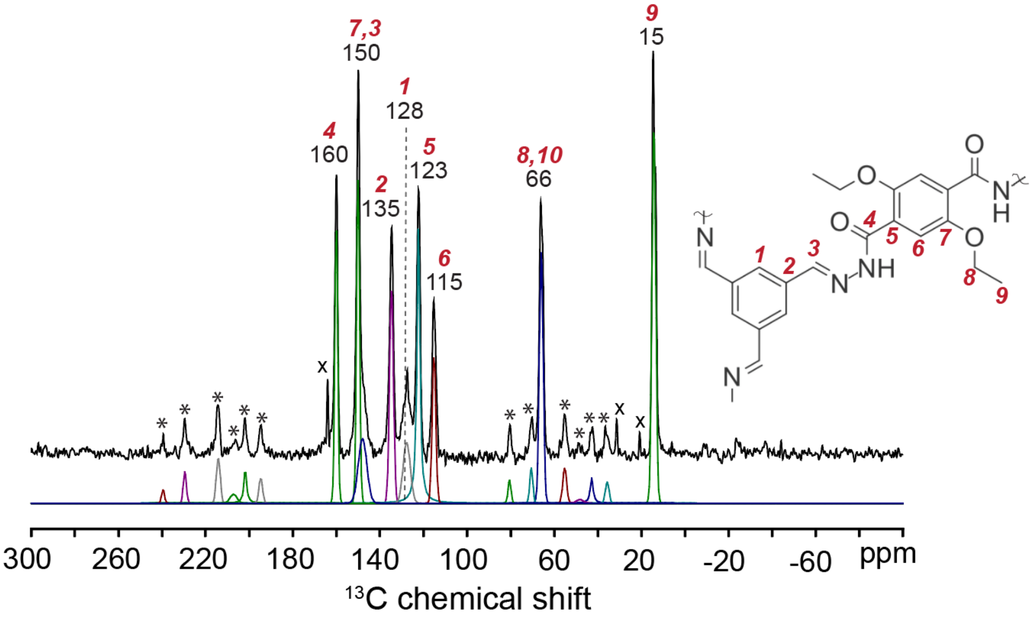

Figure S8: Spectral deconvolution of coCOF-H with spinning side-bands and solvent impurities indicated by asterisks and crosses respectively.

As shown by the 1D $^{13}C\{^1H\}$ DNP-CP MAS spectra in Fig. S9(a,b), the ^{13}C amide signal (orange band) has stronger intensity for the longest CP contact time of 5 ms. Although ^{13}C-depleted glycerol was used in the DNP solvent formulation, there is a small intensity shoulder ranging from 65 to 80 ppm from dilute amounts of ^{13}C-containing glycerol. By comparison, the 1D $^{13}C\{^1H\}$ LTMAS-CP MAS spectra in Fig. S9(c,d) were acquired on vacuum-dried 100%-amine-coCOF-H upon exposure to dry 100% ^{13}C-enriched CO_2, before and after a subsequent degassing step. As discussed in the materials section, these materials were characterized without DNP to minimally influence adsorbed CO_2. Under otherwise identical conditions, there is significantly more ^{13}C signal at 160 ppm for the material exposed to ^{13}C-enriched CO_2. In the 1D spectra the adsorbed bicarbonate (red band) and amide have overlapping signal intensity at 160 ppm, however for short contact times (500 µs) signal contributions from the amide are partially reduced.

Similarly, the 2D $^{13}C\{^1H\}$ DNP-HETCOR presented in Fig. S10a shows only weak correlated intensity from correlations between the ^{13}C amide signal (ca. 159 ppm) and ^1H aromatic signals (7.0 – 8.0 ppm). DNP-NMR can improve signal sensitivity by up to $\gamma e/\gamma_{1H} = 658$ or $\gamma e/\gamma_{15N} = 6{,}500$ for ^1H and ^{15}N nuclei respectively. Compared to Figure 6b in the main text, the 2D $^{13}C\{^1H\}$ DNP-HETCOR spectra depicted in Figure S10a has significantly improved signal-to-noise and resolves two additional ^{13}C signals at 21 and 32 ppm from residual ethoxy linker moieties. The ^{13}C signal at 159 ppm from framework amide moieties in both Figure S10a and Figure 6b exhibits weak $^{13}C\{^1H\}$-correlated intensities due to the short CP contact time (500 µs). Similarly, in Figure 6a in the main text, the absence of correlated 2D intensity associated with bicarbonate ^1H species and ^{13}C moieties (1.1% natural abundance) in the 100%-amine-coCOF-H framework is explained by the low absolute quantity of these dipolar-coupled spin pairs in comparison to the quantity of spin pairs arising from ^{13}C moieties in ^{13}C-CO_2 and 1H species in the COF framework. Importantly, as depicted in Figure S10b, DNP-NMR enables the acquisition of 1D and 2D $^{15}N\{^1H\}$ natural abundance spectra in low-N containing COF materials which would otherwise be infeasible. In Figure S10b, the tertiary amine linker moieties with ^{15}N signals at 24 and 36 ppm and the framework amide ^{15}N signal at 181 ppm are strongly correlated to ^1H signals at ca. 4.0 ppm, which arise from H_2O adsorbed in the COF pore or introduced by the DNP solvent. All five ^{15}N signals have correlated intensity with aromatic or hydrazone ^1H moieties ranging from 7 – 8 ppm. Lastly, weakly correlated $^{15}N\{^1H\}$ intensity between the amide ^{15}N signal at 181 ppm and a ^1H signal at 11.7 ppm is consistent with the ^1H chemical shift measured for compound (6). Overall, the DNP-enhanced 2D $^{13}C\{^1H\}$ and $^{15}N\{^1H\}$ HETCOR spectra confirm that the local structure of the COF framework is retained on addition of the tertiary amine linker moieties, consistent with the analyses presented in the main text.

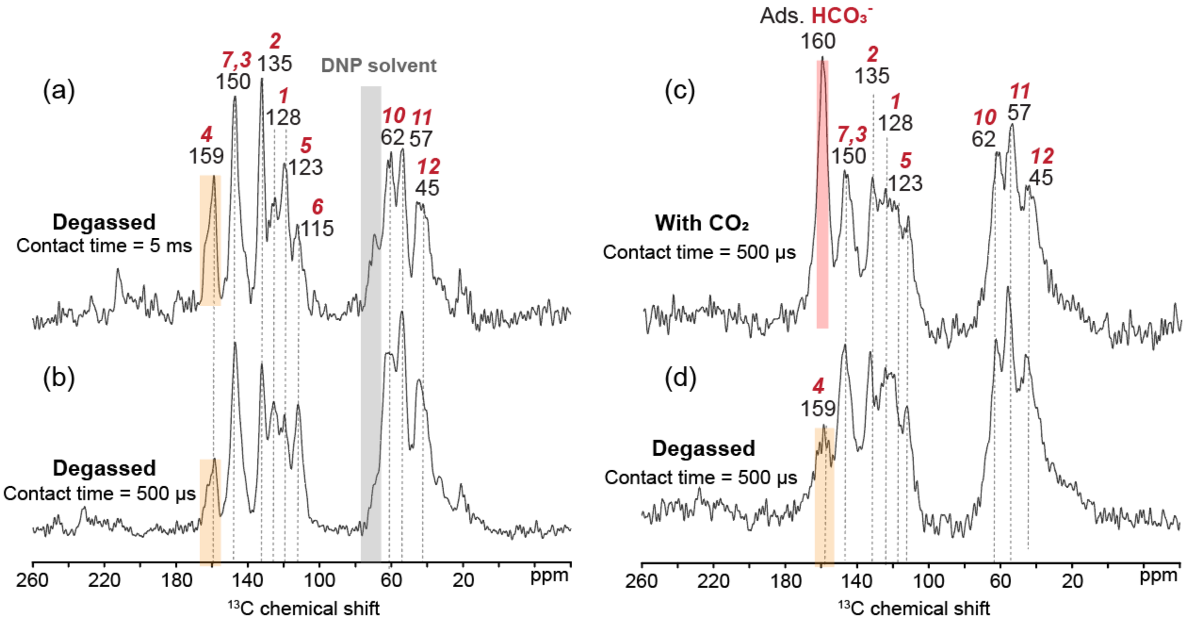

Figure S9: Vacuum dried 100%-amine-coCOF-H solid-state 1D $^{13}C\{^1H\}$ DNP-CP MAS spectra using a cross-polarization contact time of (a) 5 ms, and (b) 500 µs respectively. DNP-CP MAS spectra were acquired with 16 scans at 9.4 T, 8 kHz MAS, 95 K in the presence of 16 mM AMUPOL biradical in 60:30:10 d8-glycerol (^{13}C-depleted):D_2O:H_2O, under microwave irradiation at 263 GHz. Solid-state 1D $^{13}C\{^1H\}$ LTMAS-CP MAS spectra acquired with 256 scans and a cross-polarization contact time of 500 µs for 100%-Amine-coCOF-H (c) after exposure to 100% ^{13}C-enriched CO_2 for 12 h at 1 bar pressure and 298 K, and (d) after desorption of CO_2 for 48 h by vacuum heating at 0.1 bar and 363 K.

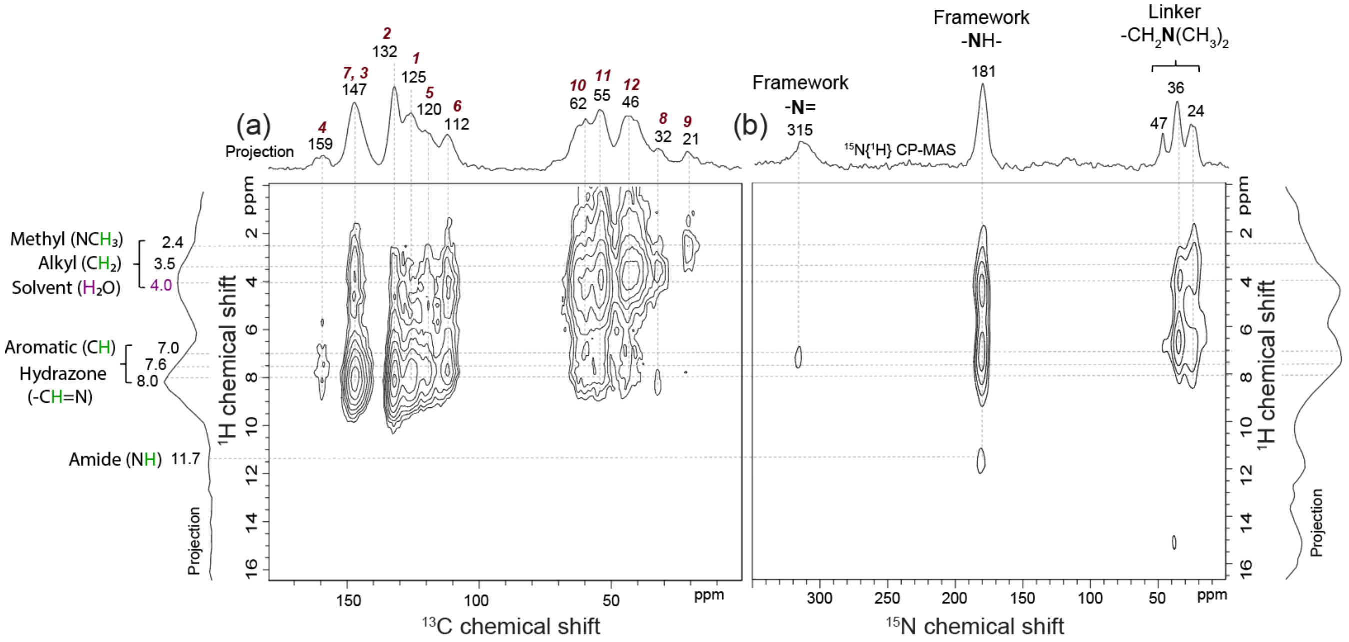

Figure S10: Vacuum-dried 100%-amine-coCOF-H (a) solid-state 2D $^{13}C\{^1H\}$ DNP-HETCOR spectra using cross-polarization contact time of 500 µs (b) and solid-state 2D $^{15}N\{^1H\}$ DNP-HETCOR spectra using cross-polarization contact time of 5 ms. The spectra were acquired at 9.4 T, 8 kHz MAS, 95 K in the presence of 16 mM AMUPOL biradical in 60:30:10 *d*₈-glycerol (^{13}C-depleted):D_2O:H_2O, under microwave irradiation at 263 GHz. With DNP sensitivity enhancements weak $^{13}C\{^1H\}$- correlated signal intensity is observed from residual pendant ethyl ether moieties in unmodified coCOF-H.

Section H. Quantum-Chemical Calculations

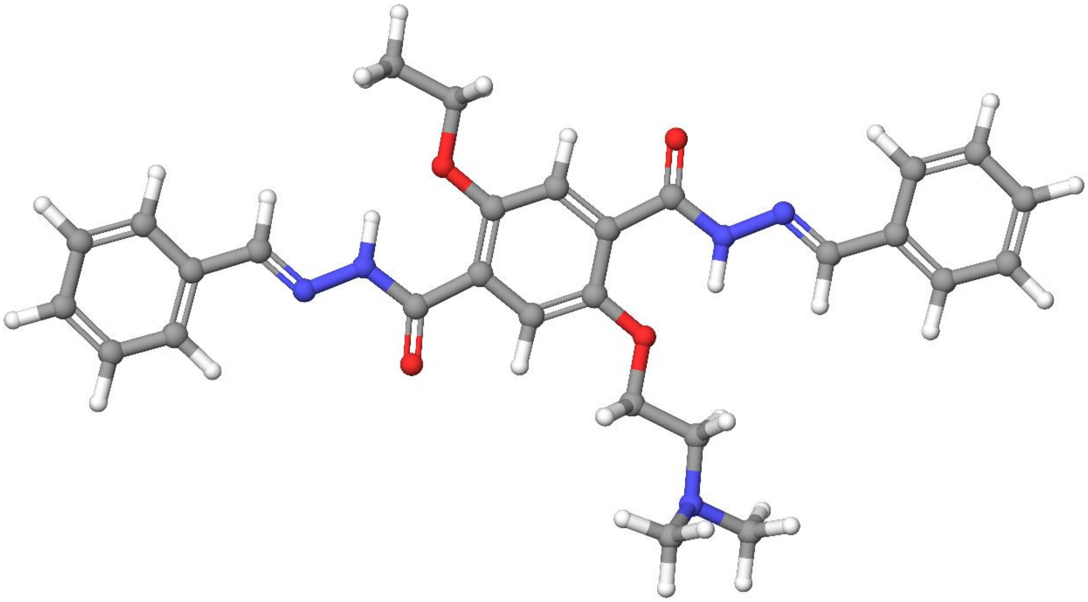

Figure S11: Optimized geometry for the DETH-M model system obtained on PBE0-D3/def2-TZVP level of theory.

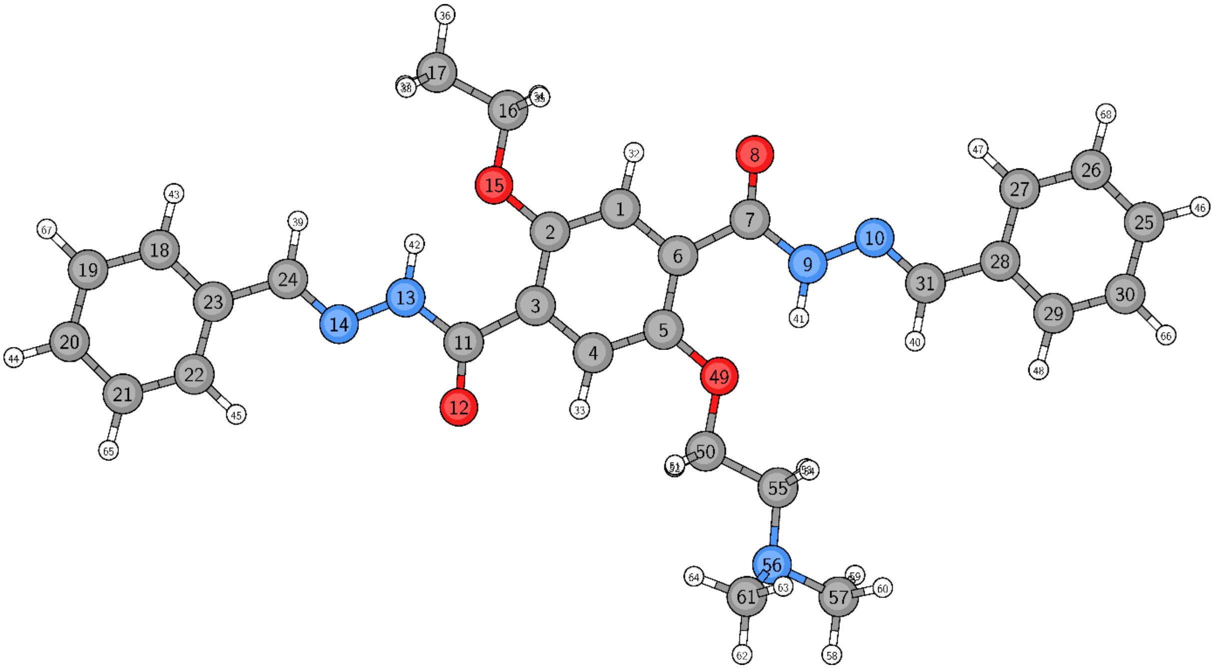

Figure S12: Atom labels for the DETH-M model system based on the optimized geometry, obtained on PBE0-D3/def2-TZVP level of theory.

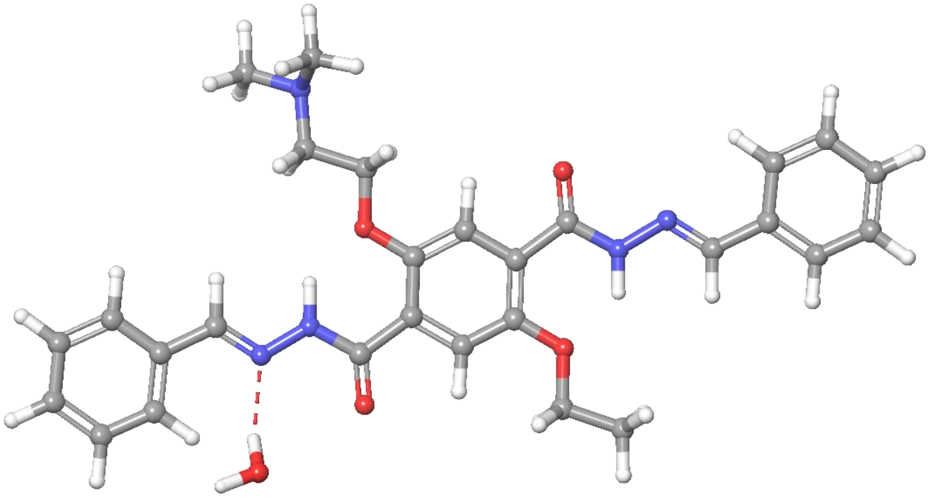

Figure S13: Optimized geometry for modeled DETH-M model system, including a single water molecule hydrogen bonded to carbonyl and imine bond, on obtained on PBE0-D3/def2-TZVP level of theory.

Table S3: Calculated ^{13}C NMR Chemical Shifts for the DETH-M model system, obtained on B97-2/pcS-2//PBE0-D3/def2-TZVP level of theory.

Atom number	Atom Type	NMR Chemical Shift [ppm]
18, 29	aromatic	137.0
23, 28	aromatic, bridge	143.5
24, 31	-CH=N-	149.3
11, 7	C=O	165.5
3, 6	central aromatic bridge	130.7
4, 1	aromatic C-H	122.9
5, 2	aromatic C-O	158.3
16	O-CH_2-	69.3
17	-CH_3	18.3
50	-O-CH_2-	72.3
55	-CH_2-**C**H_2-N-	63.1
57, 61	-N-CH_3	51.9

Table S4: Calculated ^{15}N NMR Chemical Shifts for the DETH-M model system, obtained on B97-2/pcS-2//PBE0-D3/def2-TZVP level of theory.

		NMR Chemical Shift [ppm]	
Atomnumber	Atom Type	IUPAC Nitromethan scale	liq. NH3 scale
9, 13	-NH-	-201.8	178.7
10, 14	-N=	-50.4	330.1
	-N= · H_2O	-62.0	318.5
56	-N(Me)$_2$	-367.4	13.1

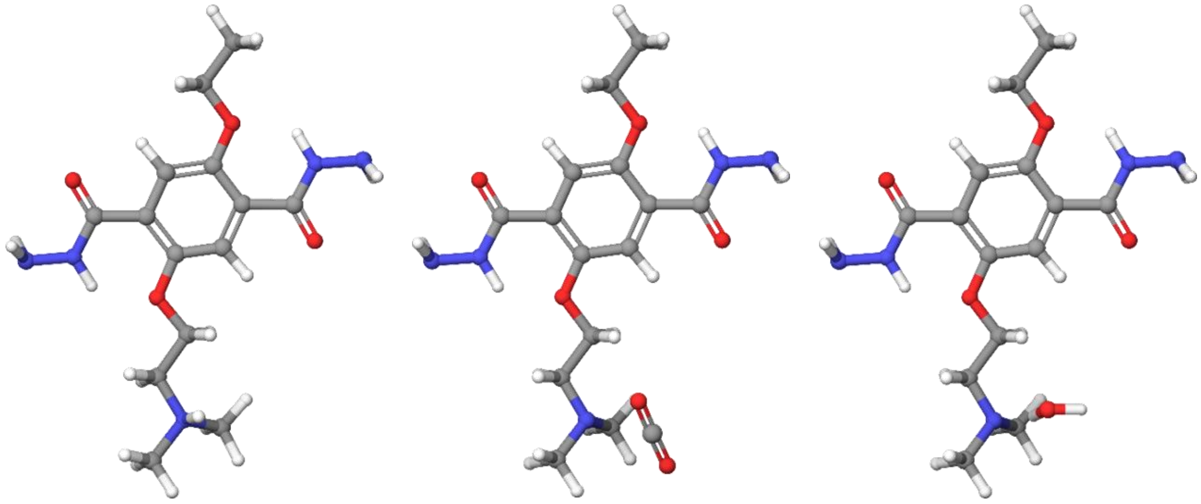

Protonated **CO_2 Physisorbate** **H_2O Physisorbate**

Figure S14: Optimized geometries for modeled DETH monomer modifications, obtained on PBE0-D3/def2-TZVP level of theory.

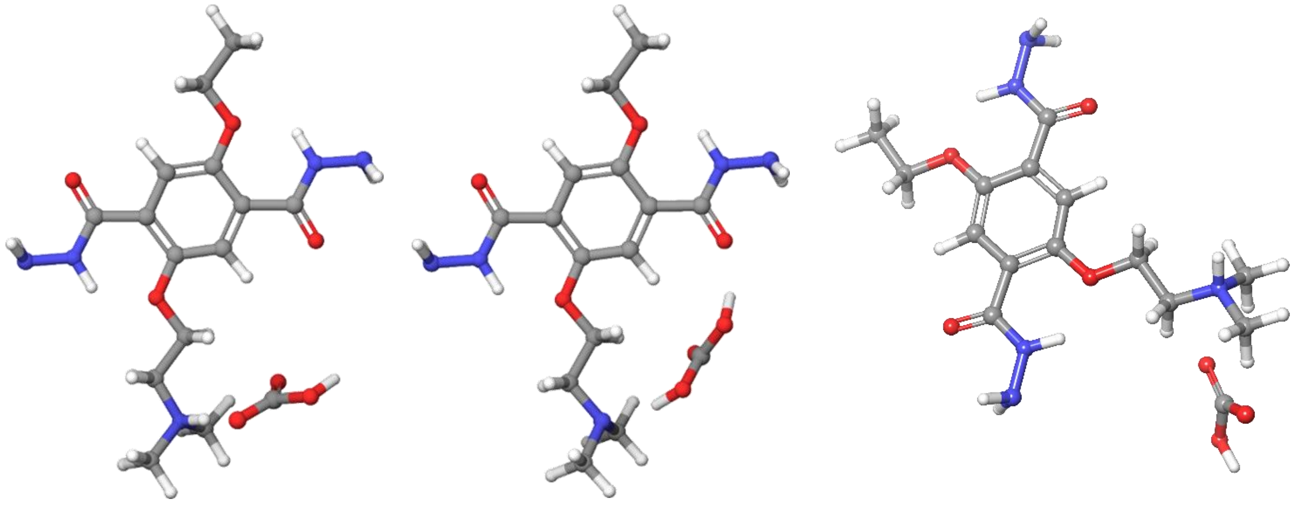

Ionic H_2CO_3 Physisorbate **Neutral H_2CO_3 Physisorbate** **Inverted H_2CO_3 Physisorbate**

Figure S15: Optimized geometries for modeled physisorbates of carbonic acid to the DETH monomer, obtained on PBE0-D3/def2-TZVP level of theory.

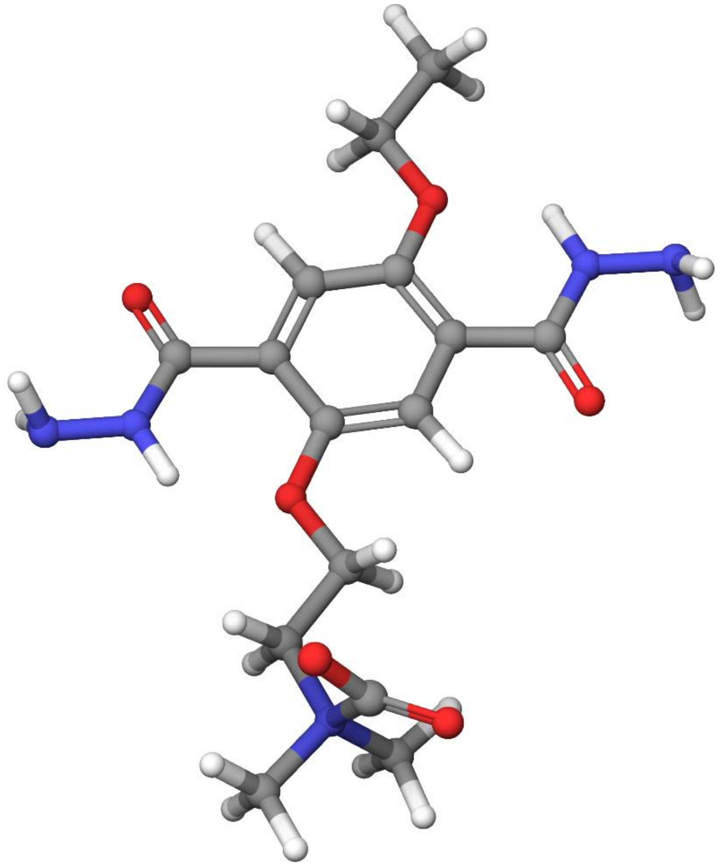

Figure S16: Optimized geometry for the modeled chemisorbate of CO_2 to the DETH monomer, obtained on PBE0-D3/def2-TZVP level of theory.

Table S5: Calculated ^{1}H NMR Chemical Shifts for the modeled DETH monomer modifications, obtained on B97-2/pcS-2//PBE0-D3/def2-TZVP level of theory.

Model	Atom Type	NMR Chemical Shift [ppm]
Ionic H_2CO_3 physisorbate	$\mathbf{H}CO3^-$	5.0
	R-N$\mathbf{H}$-$(CH_3)_2$	15.4
Neutral H_2CO_3 physisorbate	R-N-$(CH_3)_2$…$\mathbf{H}CO_3H$	11.1
	R-N-$(CH_3)_2$…$HCO_3\mathbf{H}$	10.6

Table S6: Calculated ^{13}C NMR Chemical Shifts for the modeled DETH monomer modifications, obtained on B97-2/pcS-2//PBE0-D3/def2-TZVP level of theory.

Model	Atom Type	NMR Chemical Shift [ppm]
Ionic H_2CO_3 physisorbate	$H\mathbf{C}O3^-$	171.5
Neutral H_2CO_3 physisorbate	$H_2\mathbf{C}O_3$	167.6

Table S7: Calculated ^{15}N NMR chemical shifts for the modeled DETH monomer modifications, obtained on B97-2/pcS-2//PBE0-D3/def2-TZVP level of theory.

	NMR Chemical Shift [ppm]		
	IUPAC Nitromethan scale	Liq. NH_3 scale	ΔReference
Unmodified Reference	-367.69	12.81	0.00
Protonated	-335.81	44.69	31.88
CO_2 physisorbate	-365.18	15.32	2.51
H_2O physisorbate	-363.21	17.29	4.48
Ionic H_2CO_3 physisorbate	-358.50	22.00	9.19
Neutral H_2CO_3 physisorbate	-362.52	17.98	5.16
Inverted H_2CO_3 physisorbate	-345.50	35.00	22.19
CO_2 Chemisorbate	-306.79	73.71	60.90

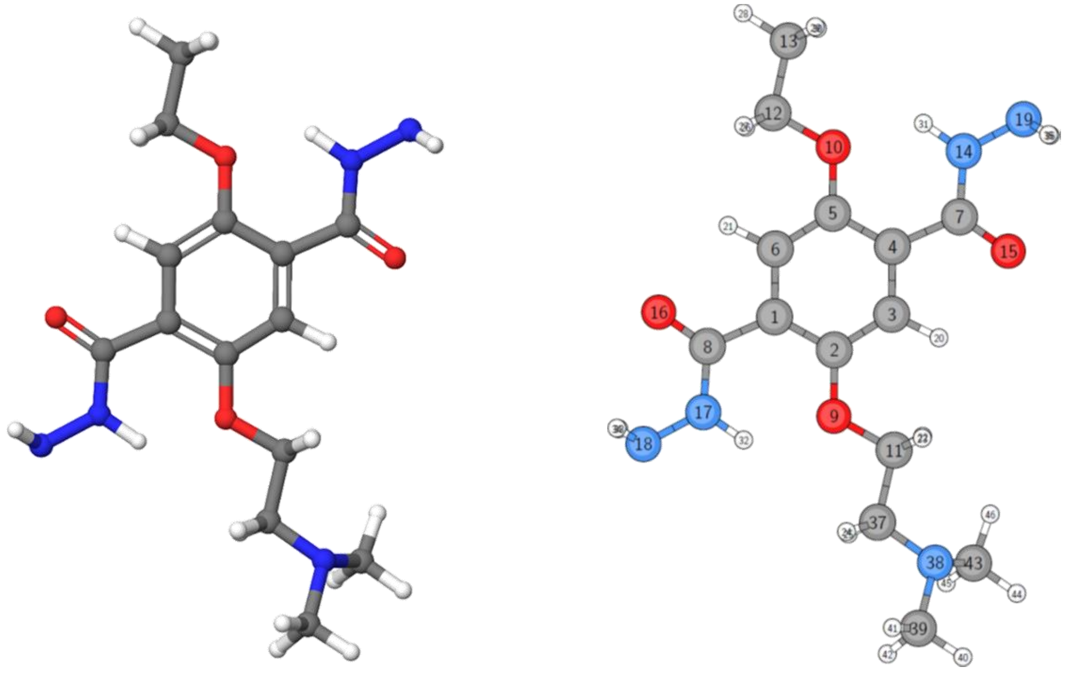

Figure S17: Optimized geometry for the DETH building block unit obtained on PBE0-D3/def2-TZVP level of theory. Corresponding atom labels are shown on the right.

Table S8: Calculated ^{15}N NMR Chemical Shifts for the DETH building block unit, obtained on B97-2/pcS-2//PBE0-D3/def2-TZVP level of theory.

		NMR Chemical Shift [ppm]	
Atom number	**Atom Type**	**IUPAC Nitromethane scale**	**liq. NH_3 scale**
14, 17	-NH-	-254.8	125.7
18, 19	$-NH_2$	-342.4	38.1
38	$-N(Me)_2$	-367.7	12.8

References

1. Wilson, P. J.; Bradley, T. J.; Tozer, D. J., Hybrid exchange-correlation functional determined from thermochemical data and ab initio potentials. *The Journal of Chemical Physics* **2001,** *115* (20), 9233-9242.
2. Jensen, F., The Basis Set Convergence of Spin−Spin Coupling Constants Calculated by Density Functional Methods. *Journal of Chemical Theory and Computation* **2006,** *2* (5), 1360-1369.
3. Perdew, J. P.; Burke, K.; Ernzerhof, M., Generalized Gradient Approximation Made Simple. *Phys. Rev. Lett.* **1996,** *77* (18), 3865-3868.
4. Grimme, S.; Antony, J.; Ehrlich, S.; Krieg, H., A consistent and accurate ab initio parametrization of density functional dispersion correction (DFT-D) for the 94 elements H-Pu. *The Journal of Chemical Physics* **2010,** *132* (15), 154104.
5. Weigend, F.; Häser, M.; Patzelt, H.; Ahlrichs, R., RI-MP2: optimized auxiliary basis sets and demonstration of efficiency. *Chem. Phys. Lett.* **1998,** *294* (1), 143-152.
6. Weigend, F., Accurate Coulomb-fitting basis sets for H to Rn. *PCCP* **2006,** *8* (9), 1057-1065.
7. *TURBOMOLE, developer version based on version V7.1 2017, a development of University of Karlsruhe and Forschungszentrum Karlsruhe GmbH, 1989-2007, TURBOMOLE GmbH, since 2007; available from http://www.turbomole.com.* .
8. Ahlrichs, R.; Bär, M.; Häser, M.; Horn, H.; Kölmel, C., Electronic structure calculations on workstation computers: The program system turbomole. *Chem. Phys. Lett.* **1989,** *162* (3), 165-169.
9. Kussmann, J.; Ochsenfeld, C., Pre-selective screening for matrix elements in linear-scaling exact exchange calculations. *The Journal of Chemical Physics* **2013,** *138* (13), 134114.
10. Kussmann, J.; Ochsenfeld, C., Preselective Screening for Linear-Scaling Exact Exchange-Gradient Calculations for Graphics Processing Units and General Strong-Scaling Massively Parallel Calculations. *Journal of Chemical Theory and Computation* **2015,** *11* (3), 918-922.